TeV γ Rays from Photodisintegration and Daughter Deexcitation of Cosmic-Ray Nuclei

Luis A. Anchordoqui,[1] John F. Beacom,[2] Haim Goldberg,[3] Sergio Palomares-Ruiz,[4,5] and Thomas J. Weiler[4]

[1]*Department of Physics, University of Wisconsin-Milwaukee, P.O. Box 413, Milwaukee, Wisconsin 53201, USA*
[2]*CCAPP, Departments of Physics and Astronomy, Ohio State University, Columbus, Ohio 43210, USA*
[3]*Department of Physics, Northeastern University, Boston, Massachusetts 02115, USA*
[4]*Department of Physics and Astronomy, Vanderbilt University, Nashville, Tennessee 37235, USA*
[5]*Institute for Particle Physics Phenomenology, University of Durham, Durham DH1 3LE, United Kingdom*

(Received 10 December 2006; revised manuscript received 3 February 2007; published 23 March 2007)

It is commonly assumed that high-energy γ rays are made via either purely electromagnetic processes or the hadronic process of pion production, followed by decay. We investigate astrophysical contexts where a third process (A^*) would dominate: namely, the photodisintegration of highly boosted nuclei followed by daughter deexcitation. Starburst regions such as Cygnus OB2 appear to be promising sites for TeV γ-ray emission via this mechanism. A unique feature of the A^* process is a sharp flattening of the energy spectrum below $\sim 10\ \mathrm{TeV}/(T/\mathrm{eV})$ for γ-ray emission from a thermal region of temperature T. The A^* mechanism described herein offers an important contribution to γ-ray astronomy in the era of intense observational activity.

DOI: 10.1103/PhysRevLett.98.121101 PACS numbers: 98.70.Rz, 98.70.Sa

In the field of TeV γ-ray astronomy, new instruments are discovering new sources at a rapid rate, both within our Galaxy and outside the Galaxy [1]. Not surprisingly, one of the brightest TeV γ-ray sources is the one discovered first, the Crab pulsar wind nebula. The integral γ-ray flux obtained from the Crab by the Whipple Collaboration is now the standard TeV flux unit: $F_{\mathrm{Crab}}(\epsilon_\gamma^{\mathrm{LAB}} > 0.35\ \mathrm{TeV}) = 10^{-10}/\mathrm{cm}^2/\mathrm{s}$ [2]. The spectral index of the Crab's integrated flux is measured to be -1.5, so F_{Crab} falls by a factor of 30 for each decade of increase in $\min(\epsilon_\gamma^{\mathrm{LAB}})$. Newly commissioned atmospheric Cherenkov telescopes (CANGAROO, HESS, MAGIC, and VERITAS) will reach a sensitivity 100 times below F_{Crab}.

Two well-known mechanisms for generating TeV γ rays in astrophysical sources [3] are the purely electromagnetic (EM) synchrotron emission and inverse Compton scattering, and the hadronic (PION) one in which γ rays originate from π^0 production and decay. There has been considerable debate over which of these two mechanisms is dominant. The mechanism for the PION mode may be either pp or $p\gamma$ collisions. In this Letter, we highlight a third dynamic which leads to TeV γ rays: photodisintegration of high-energy nuclei, followed by immediate photoemission from the excited daughter nuclei. For brevity, we label the photonuclear process $A + \gamma \to A'^* + X$, followed by $A'^* \to A' + \gamma$ ray as "A^*". It is likely that each of the three mechanisms is operative in some environments. As we show below, the A^* process is likely operative in the interesting complex environments which have accelerated nuclei and hot starlight. Fortunately, future measurements can readily distinguish among the three competing mechanisms per source. In particular, the nuclei of the A^* process act in analogy to a relativistically moving mirror [4], to "double boost" eV starlight to TeV energies for a nuclear boost factor $\Gamma_A = E_A^{\mathrm{LAB}}/m_A > 10^6$.

Nuclear photodisintegration in the astrophysical context was first calculated by Stecker in a seminal paper [5], almost 40 years ago. To our knowledge, the possibly important role of nuclear deexcitation in the astrophysical context was first appreciated and proposed by Moskalenko and collaborators [6] more than a decade ago. Since then, the A^* process has been overlooked by the γ-ray community. Now that data are becoming available that can validate or invalidate the process, it is timely to revive and further develop the A^* process. We do so by providing calculational details and by identifying the astrophysical context where this process might dominate over the EM and PION modes for production of γ rays. A detailed discussion on the main features of the EM and PION mechanisms is presented in a longer accompanying paper [7].

By far the largest contribution to the photoexcitation cross section comes from the giant dipole resonance (GDR) at $\epsilon_\gamma^{\mathrm{GDR}} \sim 10\ \mathrm{MeV}$–$30\ \mathrm{MeV}$ in the nuclear rest frame [8]. The ambient photon energy required to excite the GDR is therefore $\epsilon = \epsilon_\gamma^{\mathrm{GDR}}/\Gamma_A$. The GDR decays by the statistical emission of a single nucleon, leaving an excited daughter nucleus $(A-1)^*$. The probability for emission of two (or more) nucleons is smaller by an order of magnitude. The excited daughter nuclei typically deexcite by emitting one or more photons of energies $\epsilon_\gamma^{\mathrm{dxn}} \sim$ 1–5 MeV in the nuclear rest frame. The lab-frame energy of the γ ray is then $\epsilon_\gamma^{\mathrm{LAB}} = \Gamma_A \epsilon_\gamma^{\mathrm{dxn}}$.

As just outlined, the boost in the nuclei energy from rest to $E_A^{\mathrm{LAB}} = \Gamma_A A m_N$ plays two roles. It promotes the thermal energies of the ambient photons to the tens of MeV γ rays capable of exciting the GDR, and it promotes the deexcitation photons from a few MeV to much higher energies, potentially detectable in γ-ray telescopes. Eliminating Γ_A above leads to the relation $\epsilon\epsilon_\gamma^{\mathrm{LAB}} \sim \epsilon_\gamma^{\mathrm{GDR}}\epsilon_\gamma^{\mathrm{dxn}}$. The "$\sim$" indicates that the $\epsilon_\gamma^{\mathrm{GDR}}$ and $\epsilon_\gamma^{\mathrm{dxn}}$ energies are not sharp, but

rather distributed over their resonant shapes (''Lorentzian'' or ''Breit-Wigner''). Each of the two spectra have a width to mass ratio less than unity. It is sufficient for our purposes to treat each spectrum in the narrow-width approximation (NWA). Well-defined values for $\epsilon_\gamma^{\rm GDR}$ and $\epsilon_\gamma^{\rm dxn}$ then result. We may summarize up to this point by saying that the A^* process produces γ rays with energy $\epsilon_\gamma^{\rm LAB} = \epsilon_\gamma^{\rm GDR}\epsilon_\gamma^{\rm dxn}/\epsilon \sim 20\ {\rm TeV}/(T/{\rm eV})$ if there exists an accelerated nuclear flux with boost $\Gamma_A \sim \epsilon_\gamma^{\rm GDR}/\epsilon \sim 7 \times 10^6 (T/{\rm eV})$ or equivalent energy $E_A^{\rm LAB} \sim 7\ {\rm PeV}/(T/{\rm eV})$ per nucleon [6,9].

Here and throughout we assume a Bose-Einstein (BE) distribution with temperature T for the ambient photons; in the mean, $\langle\epsilon\rangle \sim 3T$. As an example, γ rays with energy $\epsilon_\gamma^{\rm LAB} \sim 20$ TeV are generated in this A^* process if an ambient photon temperature of an eV and a boost factor of 7×10^6 are present. Thus, we have arrived at an astrophysical environment where the A^* process may dominate production of TeV γ rays: the region must contain far-UV photons (commonly defined as 1–20 eV) from the Lyman-α emission of young, massive, hot stars such as O and B stars which have surface temperatures of $T_\star \sim$ 40 000 K (3.4 eV and $\langle\epsilon\rangle \sim 10$ eV) and 18 000 K (1.5 eV and $\langle\epsilon\rangle \sim 5$ eV), respectively; and the region must contain shocks, giant winds, or other mechanisms which accelerate nuclei to energies in excess of a PeV per nucleon. Violent starburst regions, such as the one in the direction of Cygnus, are splendid examples of regions which contain OB stars, shocks, and giant stellar winds.

With $\epsilon_\gamma^{\rm GDR}$ and $\epsilon_\gamma^{\rm dxn}$ fixed at their central values, the γ-ray spectrum $dn(\epsilon_\gamma^{\rm LAB})/d\epsilon_\gamma^{\rm LAB}$ is given by a simple Jacobian times the BE distribution with argument ϵ set to $\epsilon_\gamma^{\rm GDR}\epsilon_\gamma^{\rm dxn}/\epsilon_\gamma^{\rm LAB}$, i.e.,

$$\frac{dn(\epsilon_\gamma^{\rm LAB})}{d\epsilon_\gamma^{\rm LAB}} \propto (\epsilon_\gamma^{\rm LAB})^{-4}\left[e^{(\epsilon_\gamma^{\rm GDR}\epsilon_\gamma^{\rm dxn}/\epsilon_\gamma^{\rm LAB}T)} - 1\right]^{-1}. \quad (1)$$

Three regions in $\epsilon_\gamma^{\rm LAB}$ emerge. For $\epsilon_\gamma^{\rm LAB} < \epsilon_\gamma^{\rm GDR}\epsilon_\gamma^{\rm dxn}/T$, the γ-ray spectrum is exponentially suppressed [10]. For $\epsilon_\gamma^{\rm LAB} \gg \epsilon_\gamma^{\rm GDR}\epsilon_\gamma^{\rm dxn}/T$, there is power-law suppression. The γ-ray spectrum peaks near $\epsilon_\gamma^{\rm LAB} \sim \epsilon_\gamma^{\rm GDR}\epsilon_\gamma^{\rm dxn}/T$. In particular, one notes that the suppression of the high energy Wien end of the thermal photon spectrum has led to a similar suppression of the photon spectrum below $\epsilon_\gamma^{\rm LAB} \sim 20\ {\rm TeV}/(T/{\rm eV})$. This lower-energy suppression presents a robust prediction of the A^* process. Moreover, it contrasts greatly with the PION and EM processes, and so provides a unique signature. The A^* process predicts ''orphan'' sources, with suppression of associated GeV γ rays or MeV x rays (although the photodissociated neutrons may β-decay to neutrinos [11]). Observationally, orphan γ-ray sources have been identified [12,13], and some orphans are known to be near OB starburst regions [14].

Comparing to the PION $p\gamma$ process, the A^* process has a much lower ambient photon energy threshold; in the nuclear rest frame, the photon threshold is $\epsilon_\gamma^{\rm GDR} \sim 10$ MeV for the A^* process, but it is an order of magnitude larger at m_π for the PION $p\gamma$ process [15]. This means that for fixed ambient temperature, Γ_A need be an order of magnitude larger for the PION $p\gamma$ process, and the resulting γ-ray energies, proportional to Γ_A^2, are 2 orders of magnitude larger. The EM and PION pp processes contrast with the A^* process in that there is either no threshold (EM) or very small threshold $\mathcal{O}(2m_\pi)$ in the lab (PION pp), and the resulting γ-ray spectrum rises monotonically with decreasing $\epsilon_\gamma^{\rm LAB}$.

We now derive the rate for γ-ray production in the A^* process. The cross-section is dominated by the GDR dipole form [15], which in the NWA is

$$\sigma_A(\epsilon) \overset{\rm NWA}{\longrightarrow} \frac{\pi}{2}\sigma^{\rm GDR}\Gamma^{\rm GDR}\delta(\epsilon_\gamma^{\rm GDR} - \Gamma_A\epsilon), \quad (2)$$

where $\Gamma^{\rm GDR}$ and $\sigma^{\rm GDR}$ are the GDR width and cross section at maximum. Fitted numerical formulas are $\sigma^{\rm GDR} = 1.45A \times 10^{-27}\ {\rm cm}^2$, $\Gamma^{\rm GDR} = 8$ MeV, and $\epsilon_\gamma^{\rm GDR} = 42.65\ {\rm A}^{-0.21}$ MeV for $A > 4$ and $0.925\ {\rm A}^{2.433}$ for $A \leq 4$ [16]. The 8 MeV width implies a very short deexcitation distance of $\sim 25\Gamma_A$ fm.

The general formula for the inverse photodisintegration mean-free path (mfp) [17] for a highly relativistic nucleus with energy Γ_A/m_A propagating through an isotropic photon background with energy ϵ and spectrum $dn(\epsilon)/d\epsilon$ is [5,7]

$$(\lambda_A)^{-1} \overset{\rm NWA}{\longrightarrow} \frac{\pi\sigma^{\rm GDR}\epsilon_\gamma^{\rm GDR}\Gamma^{\rm GDR}}{4\Gamma_A^2}\int_{\epsilon_\gamma^{\rm GDR}/2\Gamma_A}^{\infty}\frac{d\epsilon}{\epsilon^2}\frac{dn(\epsilon)}{d\epsilon}. \quad (3)$$

For a nucleus passing through a region of thermal photons, integration over the BE photon distribution gives

$$(\lambda_A^{\rm BE})^{-1} \approx \frac{\sigma^{\rm GDR}\Gamma^{\rm GDR}}{\epsilon_\gamma^{\rm GDR}} n_\gamma^{\rm BE} w^2 |\ln(1 - e^{-w})|, \quad (4)$$

where we have defined a dimensionless scaling variable $w \equiv \epsilon_\gamma^{\rm GDR}/2\Gamma_A T$. From the prefactor, we learn that the peak of $(\lambda_A^{\rm BE})^{-1}$ scales in A as $\sigma^{\rm GDR}/\epsilon_\gamma^{\rm GDR} \sim A^{1.21}$, and the value of Γ_A at the peak scales as $\epsilon_\gamma^{\rm GDR} \sim A^{-0.21}$.

The scaling function $f(w) = w^2|\ln(1 - e^{-w})|$ is shown in Fig. 1. Approximations to the $|\ln|$ term yield e^{-w} for $w > 2$, and $|\ln w|$ for $w \ll 1$. Thus, the exponential suppression of the process appears again for $w > 2$, i.e., for $\epsilon_\gamma^{\rm LAB} < \epsilon_\gamma^{\rm GDR}\epsilon_\gamma^{\rm dxn}/4T$, and the small w region presents a mfp that scales as $w^2|\ln w|$. The peak region provides the smallest inverse mfp, and so this region dominates the A^* process. In the peak region, w is of order one, which implies that $\Gamma_A T \sim \epsilon_\gamma^{\rm GDR}$. When this latter relation between the nuclei boost and the ambient photon temperature is met, then the photodisintegration rate is optimized.

The area under the peak region in Fig. 1 is of order one, which leads to a simple and reasonable estimate of the inverse mfp given in Eq. (4), for any nucleus boosted near $\Gamma_A \sim \epsilon_\gamma^{\rm GDR}/T$. The useful and eminently sensible estimate is $(\lambda_A^{\rm BE})^{-1} \approx \sigma^{\rm GDR}N_\gamma^{\rm BE}$; here, we have input the typical

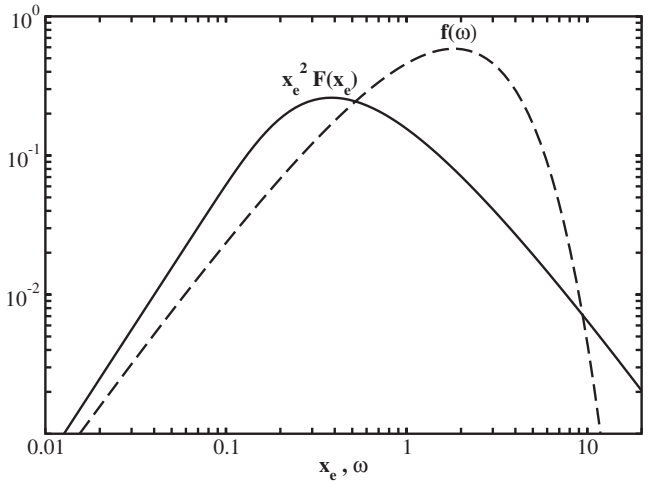

FIG. 1. The scaling functions $f(w)$ and $x_\epsilon^2 F(x_\epsilon)$, proportional to the photodissociation rate in Eq. (4) and the γ-ray $\epsilon^2 dF/d\epsilon$ spectrum in Eq. (8), respectively.

value $\Gamma^{\rm GDR}/\epsilon_\gamma^{\rm GDR} \sim 1/3$. Putting in numbers, this estimate yields

$$\lambda_A^{\rm BE} \sim \frac{5\times 10^{13}\ {\rm cm}}{A(T/{\rm eV})^3} \sim \frac{3{\rm AU}}{A(T/{\rm eV})^3} \tag{5}$$

for a nucleus with energy in the peak regime around $E_A \sim 10\ {\rm A}/(T/{\rm eV})$ PeV. Here we have used $n_\gamma^{\rm BE} = 2\zeta(3)T^3/\pi^2 \simeq T^3/4$.

An important question is how many photodisintegration steps in the nuclear chain $A \to (A-1)^* \to (A-2)^*$, etc., may be expected. Each step will produce an excited daughter which may deexcite via emission of γ rays, each having a typical lab-frame energy $\epsilon_\gamma^{\rm LAB} \sim \epsilon_\gamma^{\rm GDR}\epsilon_\gamma^{\rm dxn}/3T$. Clearly, the number of steps depends on the mfp of each excited daughter nucleus, and on the diffusion time of the nuclei in the thermal region. The probability for n cascades, producing n excited daughter nuclei and n single nucleons, may be written in symmetric ways as

$$P_n = \prod_{j=1}^{n}\int_0^{x_{j+1}} \frac{dx_j}{\lambda_j} e^{-[(x_j-x_{j-1})/\lambda_j]} = \prod_{j=1}^{n}\int_0^{x_{j+1}} \frac{dx_j}{\lambda_j} e^{-x_j\delta_j}, \tag{6}$$

where $x_0 = 0$, x_{n+1} equals the diffusion length D of nuclei in the A^* region, the ordered $x_1 \le x_2 \ldots x_n$ denote the spatial positions of successive photodisintegrations to $(A-1)^*, \ldots (A-n)^*$, $\delta_j = \lambda_j^{-1} - \lambda_{j+1}^{-1}$, and $\lambda_{n+1} = \infty$. The exponentials in (6) are probabilities that the various daughters not interact (i.e., survive) from the point of creation to the point of photodisintegration. A simple result obtains when the mfp's are long on the diffusion scale D of the A^* region. In this case the nested integrals collapse to $P_n \approx (n!)^{-1}\prod_{j=1}^n D/\lambda_j$. This is just the product of the independent probabilities for each excited daughter to be produced, times the factor $1/n!$ that divides out all but the one correct time ordering of the n photodisintegrations. One sees that, since $D/\lambda_j \ll 1$ by assumption, disintegration to more than the first excited daughter is unlikely. Such is the case if photodisintegration of nuclei occurs in the Cygnus OB starburst region, as we now demonstrate.

The aforementioned possibility of generating galactic TeV γ rays from accelerated nuclei scattering on starlight in starburst regions is of considerable astrophysical interest. The energy of the photons ($\sim 3T_\star$ in the mean) is maintained as the photons disperse from the stars, but the photon density decreases by the ratio of the surface of stellar emission ($N_\star \times 4\pi R_\star^2$) to the loss surface of the starburst region ($4\pi R_{\rm SB}^2$). Taking the giant star radius to be $R_\star \sim 10R_\odot$, the radius of the starburst region to be $R_{\rm SB} \sim 10$ pc, and the stellar count to be $N_\star \sim 2600$, the photon density is diluted by $\sim 10^{12}$. According to Eqs. (3) and (4), $(\lambda_A)^{-1}$ is proportional to the photon density, and hence to this factor. Including this factor in Eq. (5), one gets the estimate $\lambda_A \sim (56/A)(1.5\ {\rm eV}/T_\star)^3 \times 10^{23}$ cm for the nuclear mfp in the starburst region. The hot stars are dominantly (95%) B type, with $T_\star \sim 1.5$ eV. We note here that the diffusion time for a nucleus in the Cygnus OB starburst region is calculated to be $\sim 10^4$ yr $\sim 10^{22}$ cm, an order of magnitude shorter than the nuclear mfp. Accordingly, one expects only a few percent of the nuclei to photodisintegrate in the Cygnus OB region, with multiple disintegrations being rather rare.

Some early statistical-model calculations for the production of γ rays through the decay of the GDR gave a mean photon multiplicity between 0.5 and 2 for the different nuclides in the chain reaction (see Ref. [7] for details). We will simplify the data by assuming that one photon is emitted per nuclear deexcitation. Then, the rate of photoemission is just the rate of excited daughter production, which in turn is just the rate of photodisintegration. Allowing for the $1/r^2$ dilution of the γ-ray flux from the source region of volume V_{A^*} at distance d, the observed integral γ-ray flux $\mathcal{F}_\gamma$ at Earth with $\epsilon_\gamma^{\rm LAB}$ above a few TeV$({\rm eV}/T)$ is then

$$\mathcal{F}_\gamma = \frac{V_{A^*}}{4\pi d^2}\frac{1}{\lambda_A^{\rm BE}}\mathcal{F}_A, \tag{7}$$

where the flux $\mathcal{F}_A (= cn_A)$ is integral over the energy decade of the peak region, $A({\rm eV}/T){\rm PeV} < E_A < 10A({\rm eV}/T)$. It is commonly assumed that this nuclear flux results from continuous trapping of the diffuse cosmic-ray flux by diffusion in a milligauss magnetic field.

Putting into Eqs. (5) and (7) the parameters for the Cygnus OB2 region, i.e., $\lambda_A = (56/A)\times 10^{23}$ cm, $R_{\rm SB} = 10$ pc, and $d = 1.7$ kpc, one obtains $\mathcal{F}_\gamma = 2\times 10^{-10}A\mathcal{F}_A$. Thus, an accumulated nuclear flux within Cygnus OB2 of $f/{\rm cm}^2/{\rm s}$ in the PeV region gives a $\ge$ TeV γ-ray flux at Earth of $\sim 10Af \times F_{\rm Crab}(\epsilon_\gamma^{\rm LAB} \ge 1$ TeV). For example, an iron flux $\mathcal{F}_{56} = 6\times 10^{-5}/{\rm cm}^2/{\rm s}$ above a TeV leads to a γ-ray flux at Earth of about 3% of the Crab, just at the level measured by the HEGRA experiment for γ rays from the Cygnus OB2 direction [12]. In our

accompanying paper [7] we present a more detailed calculation of the A^* process for this starburst region, and show that $\mathcal{F}_{56} \sim 10^{-4}/\mathrm{cm}^2/\mathrm{s}$ is a credible 1% of the kinetic energy budget of Cygnus OB2.

The γ-ray energy spectrum remains to be discussed. In the rest frame of the excited nucleus, the photon is emitted isotropically and nearly monochromatically. Therefore, in the lab frame, the γ-ray spectrum is nearly flat between 0 and $2\Gamma_A \epsilon_\gamma^{\mathrm{dxn}}$ on a linear scale. The power spectrum and integrated power rise as $\epsilon_\gamma^{\mathrm{LAB}}$ and $(\epsilon_\gamma^{\mathrm{LAB}})^2$, respectively, peaking near $\epsilon_\gamma^{\mathrm{LAB}} \sim \epsilon_\gamma^{\mathrm{GDR}} \epsilon_\gamma^{\mathrm{dxn}}/4T \sim 10\ \mathrm{TeV}(\mathrm{eV}/T)$, as explained in the paragraph below Eq. (4).

In detail, the photon spectrum is obtained by replacing the approximate Eq. (7) with an integral over $(dF_A/dE_A^{\mathrm{LAB}}) \times (\lambda_A^{\mathrm{BE}})^{-1}$, with measure $dE_A^{\mathrm{LAB}} d\cos\theta_\gamma d\epsilon_\gamma^{\mathrm{LAB}} \delta[\epsilon_\gamma^{\mathrm{LAB}} - \Gamma_A \epsilon_\gamma^{\mathrm{dxn}}(1 + \cos\theta_\gamma)]$, where θ_γ is the angle in the nucleus rest frame between the isotropically emitted photon and the boost direction. After assuming a power law (with spectral index α) for the nuclear spectrum, and integrating over $d\cos\theta_\gamma$, one arrives at

$$\frac{(\epsilon_\gamma^{\mathrm{LAB}})^2 dF_\gamma(\epsilon_\gamma^{\mathrm{LAB}})}{d\epsilon_\gamma^{\mathrm{LAB}}} = \frac{n^{\mathrm{Th}} V_{A^*}}{4\pi d^2} \frac{\sigma^{\mathrm{GDR}} \Gamma^{\mathrm{GDR}} \epsilon_\gamma^{\mathrm{dxn}} m_N}{\epsilon_\gamma^{\mathrm{GDR}}} \times \left[\left(\frac{2E_N}{m_N}\right)^\alpha \frac{dF_N}{dE_N}\right]_{E_0} \times \left(\frac{T}{\epsilon_\gamma^{\mathrm{GDR}}}\right)^{\alpha-2} x_\epsilon^2 F(x_\epsilon), \quad (8)$$

where n^{Th} is the true density of the thermal photons after spatial dilution, E_0 is any reference energy, $x_\epsilon = \epsilon_\gamma^{\mathrm{LAB}} T/\epsilon_\gamma^{\mathrm{dxn}} \epsilon_\gamma^{\mathrm{GDR}}$ is the dimensionless energy-scaling variable, and

$$F(x_\epsilon) = \int \frac{d\omega}{\omega} \omega^\alpha f(\omega) = \int_0^{1/x_\epsilon} d\omega\, \omega^{1+\alpha} |\ln(1 - e^{-w})| \quad (9)$$

is the scaling function. Shown in Fig. 1 is $x_\epsilon^2 F(x_\epsilon)$ [18]. The γ-ray energy is $\epsilon_\gamma^{\mathrm{LAB}} = 10 x_\epsilon \mathrm{TeV} \times (\epsilon_\gamma^{\mathrm{dxn}}/\mathrm{MeV}) \times (\epsilon_\gamma^{\mathrm{GDR}}/10\ \mathrm{MeV})(T/\mathrm{eV})^{-1}$. We note that the prefactor of $x_\epsilon^2 F(x_\epsilon)$ in Eq. (8) scales in A for fixed energy per nucleon as $\sigma^{\mathrm{GDR}} \times (\epsilon_\gamma^{\mathrm{GDR}})^{-(\alpha-1)} \propto A^{1+0.21(\alpha-1)}$, while the position of the peak in the $x_\epsilon^2 F(x_\epsilon)$ spectrum at $x_\epsilon \sim 0.25$ scales mildly as $x_\epsilon \propto \epsilon_\gamma^{\mathrm{GDR}} \propto A^{-0.21}$. Well beyond the peak, the $x_\epsilon^2 F(x_\epsilon)$ spectrum falls as $x_\epsilon^{-2} \ln x_\epsilon$; equivalently, the γ-ray spectrum falls as $\approx (\epsilon_\gamma^{\mathrm{LAB}})^{-4}$.

In final summary, we have presented an alternative mechanism (A^*) for generating TeV γ rays in starburst regions. It has a unique orphanlike signature, with a flat spectrum below $\sim$20 TeV/(T/eV) and a quasi power law above. Since the EM and PION mechanisms also produce unique signatures, γ-ray astrophysics benefits from a one-to-one correspondence between the source dynamic and the observable spectrum.

We acknowledge encouragement from V. Berezinsky, useful comments from R. Ong, and grant support from NSF No. PHY-0547102 (CAREER, J. F. B), No. PHY-0244507 (H. G.), NASA No. ATP02-000-0151 (S. P. R. and T. J. W.), Spanish MCT No. FPA2005-01678 (S. P. R.), DOE No. DE-FG05-85ER40226 (T. J. W.), and Vanderbilt University Discovery Award (T. J. W.).

[1] Instruments and sources are reviewed by R. Ong, *Rapporteur Talk at the 29th International Cosmic Ray Conference* (ICRC, Pune, India, 2005), CD-Rom, and archive at http://icrc2005.tifr.res.in.
[2] G. Vacanti *et al.*, Astrophys. J. **377**, 467 (1991); A. M. Hillas *et al.*, Astrophys. J. **503**, 744 (1998).
[3] F. A. Aharonian, *Very High Energy Cosmic γ Radiation: A Crucial Window on the Extreme Universe* (World Scientific, Singapore, 2004).
[4] A. Einstein, Ann. Phys. (Leipzig) **17**, 891 (1905).
[5] F. W. Stecker, Phys. Rev. **180**, 1264 (1969).
[6] See, e.g., S. Karakula, G. Kociolek, I. V. Moskalenko, and W. Tkaczyk, Astrophys. J. Suppl. Ser. **92**, 481 (1994), and further references in our longer companion paper.
[7] L. A. Anchordoqui, J. F. Beacom, H. Goldberg, S. Palomares-Ruiz, and T. J. Weiler, astro-ph/0611581 [Phys. Rev. D (to be published)].
[8] Note that we will use ϵ for photon energies, and E for hadron and neutrino energies. It is also implicit that GDR-superscripted variables ($\epsilon_\gamma^{\mathrm{GDR}}$ here, and Γ^{GDR} and σ^{GDR} below) have an A dependence.
[9] The interesting observation that the threshold for disintegration of heavy nuclei on starlight occurs at $\sim$ PeV and so may be related to the change of slope (the ''knee'') seen in the cosmic-ray spectrum, has been noted before in J. Candia, L. N. Epele, and E. Roulet, Astropart. Phys. **17**, 23 (2002).
[10] This suppression characterizes a mean energy. However, as explained later in the text, at low energies the differential spectrum is actually flat, so the integrated power at low energy is suppressed as $(\epsilon_\gamma^{\mathrm{LAB}})^2$.
[11] L. A. Anchordoqui, H. Goldberg, F. Halzen, and T. J. Weiler, Phys. Lett. B **593**, 42 (2004).
[12] F. Aharonian *et al.* (HEGRA Collaboration), Astron. Astrophys. **431**, 197 (2005).
[13] H. Krawczynski *et al.*, Astrophys. J. **601**, 151 (2004); M. K. Daniel *et al.*, Astrophys. J. **621**, 181 (2005); M. Blazejowski *et al.*, Astrophys. J. **630**, 130 (2005).
[14] F. Aharonian *et al.* (H.E.S.S. Collaboration), Science **307**, 1938 (2005); Astron. Astrophys. **439**, 1013 (2005).
[15] F. W. Stecker and M. H. Salamon, Astrophys. J. **512**, 521 (1999); J. L. Puget, F. W. Stecker, and J. H. Bredekamp, Astrophys. J. **205**, 638 (1976).
[16] S. Karakula and W. Tkaczyk, Astropart. Phys. **1**, 229 (1993).
[17] $\lambda_A = \tau_A$ is also the mean survival time, so λ_A^{-1} is also the photodisintegration rate per nucleus.
[18] The approximate reflection symmetry in Fig. 1 between $x_\epsilon^2 F(x_\epsilon)$ and $f(w)$ about the value $x_\epsilon = w = 1/2$ is due in part to the inverse relation $x_\epsilon w = \epsilon_\gamma^{\mathrm{LAB}}/2\Gamma_A \epsilon_\gamma^{\mathrm{dxn}} = (1 + \cos\theta_\gamma)/2$, which equals 1/2 in the mean.